Environment International 131 (2019) 104971

Contents lists available at ScienceDirect

Environment International

journal homepage: www.elsevier.com/locate/envint

Corn (*Zea mays* L.): A low methylmercury staple cereal source and an important biospheric sink of atmospheric mercury, and health risk assessment

Guangyi Sun[a,b], Xinbin Feng[a,*], Runsheng Yin[c], Huifang Zhao[a,b], Leiming Zhang[d], Jonas Sommar[a], Zhonggen Li[e], Hua Zhang[a,*]

[a] *State Key Laboratory of Environmental Geochemistry, Institute of Geochemistry, Chinese Academy of Sciences, Guiyang 550002, China*
[b] *University of Chinese Academy of Sciences, Beijing 100049, China*
[c] *State Key Laboratory of Ore Deposit Geochemistry, Institute of Geochemistry, Chinese Academy of Sciences, Guiyang 550002, China*
[d] *Air Quality Research Division, Science and Technology Branch, Environment and Climate Change Canada, Toronto M3H5T4, Canada*
[e] *College of Resources and Environment, Zunyi Normal University, Zunyi 563006, China*

ARTICLE INFO

Handling Editor: Hefa Cheng

ABSTRACT

In mercury (Hg) contaminated areas of Asia, human exposure to toxic methyl-Hg (MeHg) through a rice-based diet of locally produced crop may pose a health threat. Alternative cropping system to rice in such areas would be most desirable. In this study, corn, the leading cereal source in the world with large biomass, was demonstrated to accumulate an insignificant amount of MeHg from the soil in its edible portion compared to that in rice, suggesting corn being a very competitive alternative crop. By examining Hg stable isotope composition, Hg in the aerial parts of corn was found to be mostly from the atmosphere. Maize cropping worldwide is estimated to be a discernible sink of atmospheric Hg with approximately 44 Mg Hg accumulated in each growing season on a yearly basis, most of which is from foliar uptake of atmospheric Hg and this amount is comparable to litterfall Hg observed in North America and Europe. It is thus recommended to use corn as a replacement of rice in highly Hg-contaminated areas for remediation of Hg pollution in the food supply.

1. Introduction

Mercury (Hg) is a globally distributed pollutant (Lindqvist et al., 1991). Methyl-Hg (MeHg), the primary organic Hg form in the environment, has received utmost attention due to its high neurotoxicity and capability to bioaccumulate in the food chain (Douglas et al., 2012; Zhu et al., 2018). Hg methylation occurs extensively in aquatic environments, resulting in high MeHg levels in fish by bioaccumulation of MeHg, and fish consumption is a major MeHg exposure pathway for global populations (Obrist et al., 2018). Hg methylation is also significant in paddy soils. Rice grown in Hg-contaminated areas often display high levels of MeHg, which poses potential MeHg exposure for local residents (Feng and Qiu, 2008, Zhang et al., 2010). In order to reduce the level of Hg exposure, a viable strategy for local farmers is to focus on dry land cultivation of crops with a low MeHg accumulation capability. Some studies have indicated that corn had lower MeHg bioaccumulation capability than rice (Qiu et al., 2008). However, corn can still uptake a substantial amount of inorganic Hg from either soil or atmosphere, which may pose a potential health risk to human and livestock, considering corn is an important staple worldwide.

Corn planting may be a useful approach for managing Hg pollution. Currently, the remediation technologies for Hg-contaminated soil mainly include stabilization/solidification, immobilization, vitrification, thermal desorption, nanotechnology, soil washing, electro-remediation, phytostabilization, phytoextraction and phytovolatilization (Wang et al., 2012; Cai et al., 2014; Li et al., 2019). Among these techniques, phytoextraction is a popular and environment-friendly way to reduce the content of Hg in the soil (Li et al., 2019; Pandey et al., 2019). Although it is not a Hg hyperaccumulator, corn may still have a large potential for managing Hg pollution, as corn is a typical C4 plant which makes more efficient use of available light and results in a higher photosynthetic rate and biomass production. Meanwhile, since corn is currently the world's largest cereal source, it is essential to evaluate the sources and distribution of Hg accumulated in corn to better understand its role on global Hg cycling (Beckers and Rinklebe, 2017; O'Connor et al., 2019).

* Corresponding authors.
E-mail addresses: fengxinbin@vip.skleg.cn (X. Feng), zhanghua@vip.skleg.cn (H. Zhang).

https://doi.org/10.1016/j.envint.2019.104971
Received 28 March 2019; Received in revised form 15 June 2019; Accepted 26 June 2019
Available online 05 July 2019

Hg stable isotopes have recently been used effective tracers to understand the sources and fates of Hg in the environment. The seven natural stable isotopes of Hg (with mass numbers of 196, 198, 199, 200, 201, 202 and 204) can undergo both mass-dependent (MDF, expressed as δ^{202}Hg) and mass-independent (MIF, expressed as Δ^{199}Hg, Δ^{200}Hg, and Δ^{204}Hg) isotope fractionation during complex array of Hg biogeochemical processes. Large variations in Hg isotopic compositions have been reported for natural samples (Blum et al., 2014; Yin et al., 2014). Plants receive Hg from soil and atmosphere (Yin et al., 2013), which show distinctly different Hg isotope signals (Blum et al., 2014; Yin et al., 2014). Specifically, atmospheric Hg shows more pronounced MIF signals than soil Hg. While previous studies demonstrated that large MDF occurs during Hg metabolism, significant MIF is unlikely to occur (Yin et al., 2013). The absence of MIF during metabolism suggests that MIF can be deployed as a tool to trace Hg source contribution to plants. Large variations in the MIF signals have been observed among different tissues of plants such as leaf, root, stem, and seed (Yin et al., 2013; Sun et al., 2017). Based on well-defined MIF signals of soil and atmospheric Hg sources, isotope-based binary mixing models have been used to quantify the contributions of Hg from the soil and atmospheric pool into plant tissues.

In this study, total Hg (THg) and MeHg concentrations were examined in corn grain samples collected from various provinces in China to evaluate the risk of human MeHg exposure through food consumption. In addition, isotope composition of Hg in corn tissues (leaf, root, stem, and seed) was investigated in Guizhou province, SW China to understand the sources of Hg in different corn tissues. Knowledge gained in this study provides the scientific basis for guiding future agricultural policies to minimize Hg health risk. Our results indicated that corn does not significantly accumulate MeHg from the soil in its edible portion, suggesting corn is a competitive choice for grain production, especially in Hg-contaminated areas.

2. Materials and methods

Details about the selected sites, sample preparation, and chemical analysis are provided in the Supporting information document. Briefly, corn plants were collected at one site in Hezhang zinc smelting area (HZSA), and at four sites in Wanshan mercury mining area (WMMA) namely Dashuixi (DSX), Gouxi (GX), Wukeng (WK) and Zhangjiawan (ZJW) located in Guizhou Province, SW China (Fig. S1). At each site, three individual corn plants and corresponding soils (depth: 0–20 cm) were excavated and collected. Total gaseous mercury (TGM) in the air was also measured at each site using chlorine-impregnated activated carbon traps (Fu et al., 2014; Sun et al., 2016). In addition, corn seed samples from 11 provinces (Heilongjiang, Jilin, Liaoning, Hebei, Shangdong, Henan, Shaanxi, Shanxi, Gansu, Ningxia and Inner Mongolia; Fig. S1) were purchased directly from the farmers through the Taobao e-commercial platform.

THg concentrations in soils and corn tissues were analyzed by the RA915+ Hg analyzer (Li et al., 2015). THg concentrations in the TGM trapping solutions were measured by cold vapor atomic fluorescence spectrometry (CVAFS) (Li et al., 2015). MeHg concentrations in soil and maize tissues were measured by gas chromatography - cold vapor atomic fluorescence spectrometry (GC-CVAFS) after KOH-methanol/solvent extraction, ethylation, purge-and-trap collection (Liang et al., 1996). Quality control measures included method blanks, blank spikes, matrix spikes, certified reference material (CRM) and blind duplicates. Recoveries on spiked samples were in the range of 85–120% for MeHg and 90–101% for THg. The relative percentage differences were lower than 10% for both THg and MeHg. The mean THg concentration of CRM BCR®-482 was determined at 473 ± 10 ng g^{-1} (2SD, n = 10), whereas the mean MeHg concentration of CRM TORT-2 was at 149 ± 3.5 ng g^{-1} (2SD, n = 10), which were comparable well with the certified values of 480 ± 20 ng g^{-1} and 152 ± 13 ng g^{-1}, respectively.

Hg isotope ratios were measured by a Nu-Plasma II multi-collector inductively coupled plasma mass spectrometer following the method of (Yin et al., 2010). Instrumental mass bias was corrected by standard-sample-standard bracketing using NIST SRM 3133 Hg standard with matched Hg and acid concentrations. Hg isotopic composition is reported in delta notation (δ) in units of per mil referenced to the bracketed NIST SRM 3133 Hg standard, using the following Eq. (1):

$$\delta^{xxx}Hg = \left[\frac{({}^{xxx}Hg/{}^{198}Hg)_{sample}}{({}^{xxx}Hg/{}^{198}Hg)_{NIST3133}} - 1\right] \times 1000 \tag{1}$$

MIF values are expressed by "capital delta (Δ)" notation (‰), which are the differences between the measured values and those predicted by the kinetic MDF law, using the following Eqs. (2) and (3):

$$\Delta^{199}Hg = \delta^{199}Hg_{observed} - \delta^{199}Hg_{predicted} = \delta^{199}Hg_{observed} - (\delta^{202}Hg \times 0.252) \tag{2}$$

$$\Delta^{201}Hg = \delta^{201}Hg_{observed} - \delta^{201}Hg_{predicted} = \delta^{201}Hg_{observed} - (\delta^{202}Hg \times 0.752) \tag{3}$$

The UM-Almadén secondary standard solution (n = 10) was measured for accuracy and analytical uncertainty assessment. The mean values of δ^{202}Hg, Δ^{199}Hg, and Δ^{201}Hg for UM-Almadén are −0.55 ± 0.07‰, −0.05 ± 0.08‰, and 0.04 ± 0.09‰ (2SD, n = 10), respectively, in agreement with literature data (Bergquist and Blum, 2007). Aliquots of CRM BCR 482 (n = 7) were prepared and analyzed the same way as for the samples. The δ^{202}Hg, Δ^{199}Hg, and Δ^{201}Hg of BCR 482 were determined to be −1.60 ± 0.19‰, −0.61 ± 0.08‰, and 0.60 ± 0.07‰ (2SD, n = 7), respectively, comparable with previously reported results (Estrade et al., 2010).

3. Results and discussion

3.1. THg and MeHg distribution in corn tissues

THg concentrations in soils (dry weight, dw), corn tissues (dw) and associated TGM concentration in the ambient air are summarized in

Table 1
THg and MeHg concentrations in soils (ng g^{-1}), TGM (ng m^{-3}) and corn tissues (ng g^{-1} dry weight).

	Site	n	TGM	Soils	Root	Stem	Leaf	Seed
THg	DSX	3	70 .0 ± 26.2	9607 ± 864.6	327.6 ± 124.4	72.25 ± 43.55	2412 ± 1803	13.47 ± 11.75
	GX	3	26.3 ± 11.9	15,797 ± 11,120	1113 ± 897.6	76.86 ± 44.64	926.8 ± 557.7	11.20 ± 8.94
	WK	3	53.7 ± 17.9	56,166 ± 26,653	2792 ± 1324	55.66 ± 37.75	1246 ± 1488	21.55 ± 32.67
	ZJW	3	120 ± 74.9	15,069 ± 1356	1527 ± 137.5	45.37 ± 4.083	5059 ± 455.3	9.529 ± 0.858
	HZ	3	3.10 ± 2.47	290.0 ± 26.10	28.85 ± 16.92	3.091 ± 2.243	21.61 ± 7.492	21.61 ± 7.492
MeHg	DSX	3	–	0.330 ± 0.852	0.683 ± 0.791	0.260 ± 0.354	0.153 ± 0.135	0.319 ± 0.428
	GX	3	–	0.997 ± 0.090	1.166 ± 0.799	0.079 ± 0.097	0.632 ± 0.839	0.121 ± 0.162
	WK	3	–	0.011 ± 0.0071	2.999 ± 3.589	0.161 ± 0.082	0.444 ± 0.715	0.054 ± 0.016
	ZJW	3	–	0.504 ± 0.045	6.164 ± 4.554	0.068 ± 0.094	0.144 ± 0.059	0.074 ± 0098
	HZ	3	–	0.015 ± 0.034	0.071 ± 0.092	0.001 ± 0.016	0.060 ± 0.034	0.013 ± 0.056

Table 1. THg concentration in soils from the WMMA sites ranged from 0.29 to 69.5 μg g^{-1} with the majority of samples well above the national soil quality standard of China (1.5 μg g^{-1}). Soils from HZSA displayed a much lower and more confined range of THg concentrations from 0.15 to 0.34 μg g^{-1}. The mean TGM concentrations observed at all the WMMA sites were > 10 times higher than the regional background level (2.80 ± 1.51 ng m^{-3}, Fu et al., 2012), specifically, ZJW (120 ± 74.9 ng m^{-3}) > DSX (70 ± 26.2 ng m^{-3}) > WK (53.7 ± 17.9 ng m^{-3}) > GX (26.3 ± 11.9 ng m^{-3}), while that at HZSA (3.10 ± 2.47 ng m^{-3}) was only slightly elevated above the regional background level. At the WK, ZJW and DSX sites, the mean THg concentrations in maize tissues exhibited the following decreasing order of leaf > root > stem > seed, while at the GX and HZ sites, a slightly different order was observed with the highest mean THg concentrations in root, followed by leaf, stem, and seed. Note that much higher Hg contents in leaf and root than stem and seed were also previously observed in locally cultivated rice (Yin et al., 2013). The Pearson correlation matrix for THg concentrations of corn tissues, soil and TGM is illustrated in Table S1. Using a two-tailed *t*-test, significant ($p < 0.01$) correlations were obtained between THg concentrations of root and soil and between TGM in air and THg in leaf, indicating that soil is the major source of Hg in root, and leaf mainly receives Hg from the atmosphere (Zhang et al., 2010; Meng et al., 2010). Significant positive correlations were also observed between TGM and THg in root ($p < 0.05$), and between TGM and THg in stem ($p < 0.01$), indicating atmospheric Hg is the major source of Hg in aerial parts of corn plant. Root Hg concentrations showed insignificant correlations ($p > 0.05$) with stem and leaf, suggesting that the transport of Hg from root to leaf is limited, consistent with previous conclusions (Bishop et al., 1998; Niu et al., 2011). In addition, the correlations obtained between THg concentrations of root and that of soil ($p < 0.01$) were more positive than that between TGM and THg in soil (0.496, $p < 0.05$) and between TGM in air and THg in the root (0.463, $p < 0.05$). The positive correlation between TGM and THg in soil implies that the emission of Hg(0) from the soil is the major source of TGM in the studied area. As root receives the majority of its Hg from the soil, the positive correlation between root Hg and TGM may be simply explained by the positive correlation between TGM and THg in soil.

3.2. Hg isotopes suggest atmospheric Hg as the major Hg source in maize

Hg isotopic composition of soils, TGM and maize tissues are shown in Fig. 1 and Table S2. Soils displayed the highest δ^{202}Hg values ranging from −2.38 to 0.72‰. Most of the soil samples had an insignificant MIF signal (Δ^{199}Hg ~ 0‰), except soils at GX that displayed slightly positive Δ^{199}Hg values (0.13 ± 0.05‰). TGM samples at GX were characterized by negative δ^{202}Hg values (daytime: −1.77 ± 0.20‰; night-time: −1.33 ± 0.15‰) and slightly positive Δ^{199}Hg values (daytime: 0.18 ± 0.02‰; night-time: 0.12 ± 0.01‰). TGM samples at WK showed negative δ^{202}Hg values (−1.45 ± 1.29‰) but a diminished MIF signal (Δ^{199}Hg: -0.09 ± 0.01‰). Overall, the isotopic signals of TGM in corn canopies of this study differ substantially from those in previous observations (δ^{202}Hg: −2.32 to −2.14‰; Δ^{199}Hg −0.34 to −0.30‰) made over rice paddies at the GX and WK sites (Yin et al., 2013). Yin et al. (2013) attributed the relatively negative MIF values of gaseous Hg in the air to substantial photo-reduction of Hg(II) in paddy waters releasing of Hg(0) with significantly negative Δ^{199}Hg values. Significantly negative Δ^{199}Hg values were also reported in TGM samples collected from Wisconsin forests (Demers et al., 2013). A plausible explanation for the lack of significantly negative Δ^{199}Hg signal in our TGM samples is that photo-reduction of soil Hg(II) and subsequent Hg(0) volatilization were curbed in the final vegetative stage of corn croplands. In a study on the North China Plain, (Sommar et al., 2016) showed that Hg(0) uptake by the corn canopy at this stage may offset ground Hg(0) emission with additional removal of Hg(0) from the atmosphere.

Underneath the developed corn canopy with low light penetration, photo-reduction became less important and thus microbial reduction became more important. In turn, microbial reduction of soil Hg released Hg(0) with more negative δ^{202}Hg but without triggering discernible MIF. Analogously, atmospheric Hg(0) uptaken by plant shifted towards higher δ^{202}Hg values. Our TGM samples showed similar Δ^{199}Hg values to the underlying soil, therefore the enhancement in surficial TGM in dense corn canopies by soil Hg(0) efflux plausibly stem from a pool mainly reduced by non-photochemical processes (e.g., microbial reduction, volatilization). This study contrasted with co-located observations for a succession of years in the past decade suggesting a rapidly declining trend in TGM of WMMA since mining operation was officially closed in 2005 (Wang et al., 2007; Li et al., 2009; Meng et al., 2010; Dai et al., 2012; Yin et al., 2013; Zhao et al., 2016). It could be hypothesized that TGM isotopic signal reflects its source pattern and therefore displays a concentration dependence. Consequently, it could not be excluded that the differing TGM isotopic signal observed by Yin et al. (2013) associated with a higher average TGM level (GX: 211.3 ± 19.1 ng m^{-3}; DSX 57.9 ± 11.3 ng m^{-3}) might reflect not only the effects of paddy farming but also the more distant sources that since then has been curbed by remediation efforts. Verification of this hypothesis requires more data of the TGM isotopic composition variations in WMMA.

Overall, δ^{202}Hg values in the investigated corn tissues span over a

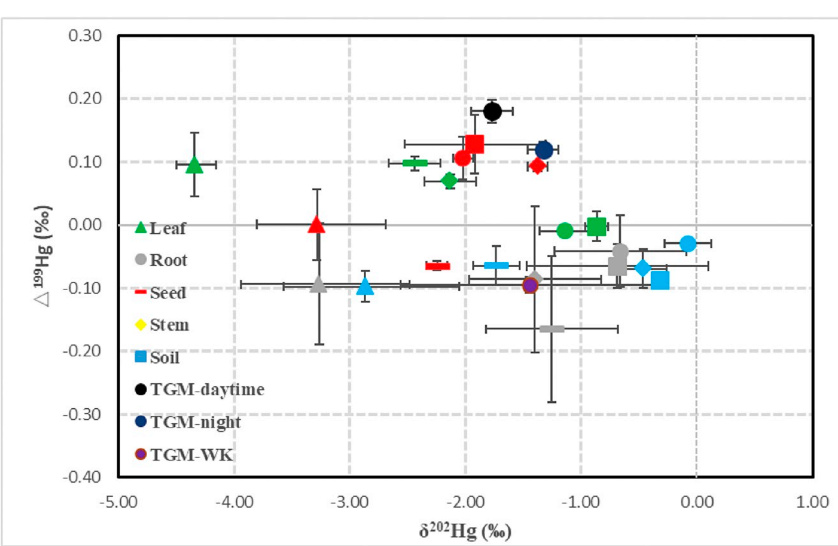

Fig. 1. Δ^{199}Hg versus δ^{202}Hg for TGM, soil and maize tissues. Note: Sampling sites ZJW, GX, DSX, and WK are marked green, red, gray and, blue, respectively. Error bars represent the 2SE of Δ^{199}Hg and δ^{202}Hg for all the samples collected from the same site. (For interpretation of the references to color in this figure legend, the reader is referred to the web version of this article.)

wide range exceeding 4.5‰ (−4.49 to 0.03‰). In WMMA, leaf samples showed the lowest mean δ^{202}Hg, followed by seeds, stems and roots. In HZSA, however, seeds had the lowest δ^{202}Hg compared to leaves, stems and roots. For the WMMA sites, isotopic MDF distribution pattern of maize samples unanimously mimics the pattern previously observed in rice (Yin et al., 2013). Soils and TGM samples among all the sites had higher δ^{202}Hg than corn tissues (Fig. 1). This can be explained by the fact that kinetic MDF occurs during incorporation of soil and atmospheric Hg by plants. Pearson correlation analysis suggests that root mainly received Hg from the soil while leaves mainly received Hg from the atmosphere. Previous studies have suggested that significant MIF is unlikely to occur during metabolic processes (Blum and Bergquist, 2007; Yin et al., 2013). In the present study, all leaves showed lower Δ^{199}Hg values than TGM samples, indicating corn leaves also received Hg(0) with negative Δ^{199}Hg values outside of the maize fields. Yin et al. (2013) reported that negative Δ^{199}Hg (−0.34 to −0.30‰) in TGM samples from paddy fields in WMMA may be a potential Hg source of Hg in maize leaves. The Δ^{199}Hg of our leaves fall between the Δ^{199}Hg values of our TGM samples and those collected by Yin et al. (2013). Different from what was found in Yin et al. (2013), however, no significant differences in Δ^{199}Hg values were observed among aerial part tissues of corn. The lack of significant differences in Δ^{199}Hg values suggests that Hg in ground tissues were mainly from the atmosphere. This finding differentiates maize from rice, because a substantial fraction of Hg in rice seed is soil-derived (Yin et al., 2013).

3.3. MeHg exposure risk for corn consumption

All the corn seeds (including those collected from Hg polluted sites such as HZSA and WMMA) have extremely low MeHg levels (< 0.01 to 1.36 ng g^{-1}, dw, Table 1) with a mean MeHg concentration of only 0.20 ± 0.34 ng g^{-1} (2SD, n = 48), which is much lower than MeHg in rice (1.6–9.3 μg g^{-1}), vegetables (0.023–2.5 μg g^{-1}), meat (0.26–0.85 μg g^{-1}) and poultry (0.56–2.4 μg g^{-1}) (Zhang et al., 2010). In HZSA and WMMA, MeHg concentrations in corn tissues decrease roughly in the order of root > leaf > stem > seed. This is completely different from what was observed in rice, which showed seed having the highest MeHg levels compared to the other tissues (Zhang et al., 2010). Corn contains much lower MeHg fractions than rice does, suggesting a low bioaccumulation capability of MeHg by corn and/or a low MeHg production in soil.

The human consumption of corn in China amounted for 18.0 million tons in 2014 (Zhang, 2016), equivalent to a daily intake of roughly 37 g per capita. In the same year, roughly 110.8 million tons of corn were used domestically for feeding pigs (FAOUN, 2017). The pork consumption in China was previously been estimated at 17.6 kg person^{-1} year^{-1} (W. Tang, 2013; Q.P. Tang, 2013). Based on the MeHg concentrations in corn, we calculated the Chronic Daily Intake (CDI) values for the general adult population (USEPA, 1989), using the average daily intake (CDI) (mg kg^{-1} day^{-1}) method (Eq. (4)):

$$CDI = (C \times IR \times EF \times ED)/(BW \times AT) \tag{4}$$

where CF is MeHg concentrations in corn seed or pork (mg kg^{-1}), IR is the ingestion rate (kg person^{-1} day^{-1}), EF is the exposure frequency, ED is the exposure duration, BW is the average body weight, and AT is the average exposure time. The daily intake of THg and MeHg for maize and pork were calculated by considering the concentrations observed in this study and the enrichment coefficient of corn-pork (for MeHg) (W. Tang, 2013). The parameters used in the risk assessment are summarized in Table S3. The estimated CDI (Fig. 2) of corn and pork fed with corn at all the sites are below 0.1 μg kg^{-1} bw day^{-1} reference dose (RfD). The results suggest that the health risk of MeHg through corn consumption, directly and indirectly, is low in China, and highlight the benefit of corn planting for decreasing the human MeHg exposure risk in the future.

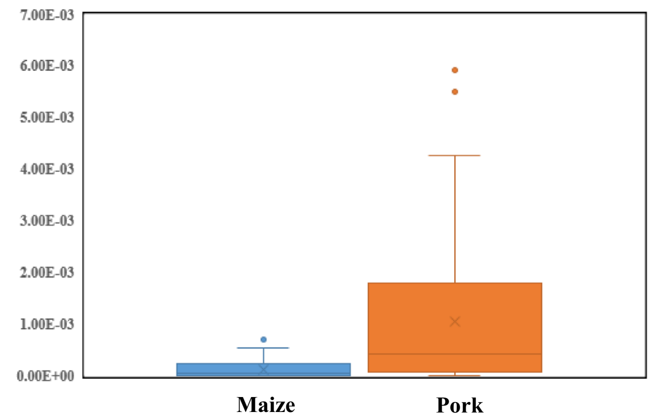

Fig. 2. CDI of MeHg in corn and pork.

3.4. Corn plant as an important sink of atmospheric Hg

Due to the large biomass of corn and Hg in corn materials being basically entirely from the atmosphere, corn plants may remove a substantial amount of Hg from the atmosphere. In the present study, THg concentrations of maize leaves are positively correlated with the TGM concentrations (Fig. S2), providing a way of predicting THg concentrations in maize leaves based on known TGM concentrations of the growing area (Temmerman et al., 2009; Zheng et al., 2018) . The average TGM concentrations in southern and northern hemispheres were previously estimated to be 0.8–1.1 ng m^{-3} and 1.7 ng m^{-3}, respectively (Obrist et al., 2018; Fu et al., 2012). Excluding Brazil, the world's major corn production areas are concentrated in the northern hemisphere, and thus 1.7 ng m^{-3} was chosen as the atmospheric concentration. Using the correlation in Fig. S2, corn leaves in the world were predicted to have THg concentrations of 59.4 ng g^{-1} (dry weight). The biomass of corn leaves was previously estimated to be 54.6 ± 14.1 g per plant and 3.3 ± 0.9 Mg/ha, and corn planning areas cover 2.27 × 10^{8} ha (National Bureau of Statistics of China, 2015; FAOUN, 2017). Therefore, the biomass of corn leaves in the world is 7.43 × 10^{8} Mg. Multiplying the predicted THg concentrations of corn tissues (leaf) by their biomass, corn planting was estimated to result in the incorporation of 44 Mg of Hg from the atmosphere in each growing season. In addition, ~19.4 μg m^{-2} year^{-1} Hg uptaken by leaves in each growing season was comparable to the deposition fluxes (μg m^{-2} year^{-1}) of Hg through litterfall in North America and Europe (Fisher and Wolfe, 2012; Juillerat et al., 2012; Fu et al., 2016). Note that corn only has three months of the growing period. The high capability of incorporating atmospheric Hg by corn plants may be of particular importance in remediation of atmospheric Hg in contaminated areas. Taken WMMA as an example, the mean THg concentration of mature corn foliage is ~3 μg g^{-1}, which means that about 10 g Hg could be absorbed by corn leaves per hectare in each growing season (about 100 days). Note that in the background areas, the absorption coefficient of atmospheric mercury by maize leaves is only 8.2 (Liu et al., 2004; Wang et al., 2017; Fu et al., 2012) because of the low atmospheric mercury concentrations.

4. Conclusions

Although fish and seafood are the most common dietary sources of toxic methylmercury worldwide, rice, a staple food for billions, can also be a predominant source of methylmercury in mercury-contaminated areas of Asia. Thus, in the context of the Minamata Convention, risk control based on alternative cropping systems to rice in such areas would be most desirable. In addition, it is an urgent task and huge challenge to reduce the local mercury pollution in a sustainable, simple and economical way. Results from this study indicated that corn insignificantly accumulate MeHg from soil in its edible portion, contrary to what rice does, suggesting corn is a very competitive alternative choice for grain production. At the same time, corn has a variety of economic values, such as human consumption, livestock farming and bio-fuel. It is recommended to use corn as a suitable crop during agricultural planting structure adjustment in highly Hg-contaminated areas. This study only investigated samples of final growth stage (mature) of corn and more research may be needed during other growing stages for better understanding migration and transformation of mercury in this type of ecosystem. Results gained in this study should also be validated in other regions with mercury-contaminated soils.

Declaration of Competing Interest

The authors declare no competing financial interest.

Acknowledgments

This study was funded by the Strategic Priority Research Program of Chinese Academy of Sciences, Pan-Third Pole Environment Study for a Green Silk Road (Pan-TPE, XDA20040502), China Postdoctoral Science Foundation (2018M640939), the Bureau of Frontier Sciences and Education, Chinese Academy of Sciences (grant no. QYZDJSSW-DQC005-02), the National Science Foundation of China (grant nos. 41773146), and K. C. Wong Education Foundation.

Appendix A. Supplementary data

Site description; sample collection; sample analytical procedure; supplementary figures and tables. Supplementary data to this article can be found online at https://doi.org/10.1016/j.envint.2019.104971.

References

Beckers, F., Rinklebe, J., 2017. Cycling of mercury in the environment: sources, fate, and human health implications - a review. Crit. Rev. Environ. Sci. Technol. 47, 693–794.
Bergquist, B.A., Blum, J.D., 2007. Mass-dependent and independent fractionation of Hg isotopes by photoreduction in aquatic systems. Science 318, 19.
Bishop, C.A., Ng, P., Pettit, K.E., Kennedy, S.W., Stegeman, J.J., Norstrom, R.J., Brooks, R.J., 1998. Environmental contamination and developmental abnormalities in eggs and hatchlings of the common snapping turtle (Chelydra serpentina serpentina) from the Great Lakes—St Lawrence River basin (1989–1991). Environ. Pollut. 101 (1), 143–156.
Blum, J.D., Bergquist, B., 2007. A reporting of variations in the natural isotopic composition of mercury. Anal. Bioanal. Chem. 388, 353–359.
Blum, J.D., Sherman, L.S., Johnson, M.W., 2014. Mercury isotope in earth and environmental sciences. Annu. Rev. Earth Planet. Sci. 42, 249–269.
Cai, M.F., Li, K.M., Xie, D.P., et al., 2014. The status and protection strategy of farmland soils polluted by heavy metals. Environ. Sci. Technol. 37 (120), 223–230.
Dai, Z.H., Feng, X., Sommar, J., Li, P., Fu, X., 2012. Spatial distribution of mercury deposition fluxes in Wanshan Hg mining area, Guizhou province, China. Atmos. Chem. Phys. 12 (14), 6207–6218.
Demers, J.D., Blum, J.D., Zak, D.R., 2013. Mercury isotopes in a forested ecosystem: implications for air-surface exchange dynamics and the global mercury cycle. Glob. Biogeochem. Cycles 27, 222–238.
Douglas, T.A., Loseto, L.L., Macdonald, R.W., Outridge, P., Dommergue, Aurélien, Poulain, A., et al., 2012. The fate of mercury in arctic terrestrial and aquatic ecosystems, a review. Environ. Chem. 9 (4), 321–355.
Estrade, N., Carignan, J., Sonke, J.E., Donard, O.F.X., 2010. Measuring Hg isotopes in Bio-Geo_Environmental reference materials. Geostand. Geoanal. Res. 34, 79–93.
Feng, X.B., Qiu, G.L., 2008. Mercury pollution in Guizhou, Southwestern China - an overview. Sci. Total Environ. 400 (400), 227–237.
Fisher, L.S., Wolfe, M.H., 2012. Examination of mercury inputs by throughfall and litterfall in the Great Smoky Mountains National Park. Atmos. Environ. 554–559.
Food and Agriculture Organization of the United Nations (FAOUN), 2017. Food and agriculture data. http://www.fao.org/faostat/en/#home.
Fu, X.W., Feng, X.B., Sommar, J., Wang, S.F., 2012. A review of studies on atmospheric mercury in China. Sci. Total Environ. 421-422, 73–81.
Fu, X.W., Heimbuerger, L.E., Sonkem, J.E., 2014. Collection of atmospheric gaseous mercury for stable isotope analysis using iodine and chlorine impregnated activated carbon traps. J. Anal. At. Spectrom. 29, 841–852.
Fu, X.W., Yang, X., Lang, X.F., Zhou, J., Zhang, H., Yu, B., Yang, H.Y., Lin, C.L., Feng, X.B., 2016. Atmospheric wet and litterfall mercury deposition at urban and rural sites in China. Atmos. Chem. Phys. 16, 11547–11562.
Juillerat, J.I., Ross, D.S., Bank, M.S., 2012. Mercury in litterfall and upper soil horizons in forested ecosystems in Vermont, USA. Environ. Toxicol. Chem. 31 (8), 1720–1729.
Li, P., Feng, X., Qiu, G., Shang, L., Wang, S., Meng, B., 2009. Atmospheric mercury emission from artisanal mercury mining in Guizhou Province, Southwestern China. Atmos. Environ. 43 (14), 2247–2251.
Li, P., Feng, X.B., Chan, H.M., Zhang, X.F., Du, B.Y., 2015. Human body burden and dietary methylmercury intake: the relationship in a rice-consuming population. Environ. Sci. Technol. 49 (16), 9682–9689.
Li, C.F., Zhou, K.H., Qin, W.Q., et al., 2019. A review on heavy metals contamination in soil: effects, sources, and remediation techniques. Soil Sediment Contam. 28 (4), 380–394.
Liang, L., Horvat, M., Cernichiari, E., Gelein, B., Balogh, S., 1996. Simple solvent extraction technique for elimination of matrix interferences in samples by ethylation gas chromatography cold vapor atomic fluorescence spectrometry. Talanta. 43, 1883–1888.
Lindqvist, O., et al., 1991. Mercury in the Swedish environment - recent research on causes, consequences and corrective methods. Water Air Soil Pollut. 55 (1–2), R11.
Liu, R.H., Wang, Q.C., Lu, X.G., et al., 2004. Distribution and stock of mercury in typical wetland plant in the Sanjiang plain. Chin. J. Appl. Ecol. 15 (2), 287–290.
Meng, B., Feng, X.B., Qiu, G.L., Cai, Y., Wang, D.Y., Li, P., Shang, L.H., Sommar, J., 2010. Distribution patterns of inorganic mercury and methylmercury in tissues of rice (Oryza sativa L.) plants and possible bioaccumulation pathways. J. Agric. Food Chem. 58 (8), 4951–4958.
National Bureau of Statistics of China (NBSC), 2015. http://data.stats.gov.cn/search.htm?s=corn.
Niu, Z.C., Zhang, X.S., Wang, Z.W., Ci, Z.J., 2011. Field controlled experiments of mercury accumulation in crops from air and soil. Environ. Pollut. 159, 2684–2689.
Obrist, D., Kirk, J.L., Zhang, L., Sunderland, E.M., Jiskra, M., Selin, N.E., 2018. A review of global environmental mercury processes in response to human and natural perturbations: changes of emissions, climate, and land use. Ambio 47, 116–140.
O'Connor, et al., 2019. Mercury speciation, transformation, and transportation in soils, atmospheric flux, and implications for risk management: a critical review. Environ. Int. 126, 747–761.
Pandey, J., Verma, R.K., Singh, S., 2019. Suitability of aromatic plants for phytoremediation of heavy metal contaminated areas: a review. Int. J. Phytoremediation 21 (5), 405–418.
Qiu, G.L., Feng, X.B., Li, P., Wang, S.F., Li, G.H., Shang, L.H., Fu, X.W., 2008. Methylmercury accumulation in rice (Oryza sativa L.) grown at abandoned mercury mines in Guizhou, China. J. Agric. Food Chem. 56 (7), 2465–2468.
Sommar, J., Zhu, W., Shang, L., Lin, C.J., Feng, X., 2016. Seasonal variations in metallic mercury (Hg0) vapor exchange over biannual wheat–corn rotation cropland in the North China Plain. Biogeosciences 13, 2029–2049.
Sun, G.Y., Sommar, J., Feng, X.B., Lin, C.J., Ge, M.F., Wang, W.G., Yin, R.S., Fu, X.W., Shang, L.H., 2016. Mass-dependent and independent fractionation of mercury isotope during gas-phase oxidation of elemental mercury vapor by atomic Cl and Br. Environ. Sci. Technol. 50 (17), 9232–9241.
Sun, L.M., Lu, B.Y., Yuan, D.X., Hao, W.B., Zheng, Y., 2017. Variations in the isotopic composition of stable mercury isotopes in typical mangrove plants of the Jiulong estuary, SE China. Environ. Sci. Pollut. Res. 24 (2), 1459–1468.
Tang, W., 2013a. Mercury Pollution Characteristic in Typical Mercury Sources in China and Health Risk. Donghua University (Master's dissertation).
Tang, Q.P., 2013b. A Study on China's Food Security on the Views of Diet Structure. Jinan University Press.
Temmerman, L.D., Waegeneers, N., Claeys, N., Roekens, E., 2009. Comparison of concentrations of mercury in ambient air to its accumulation by leafy vegetables: an important step in terrestrial food chain analysis. Environ. Pollut. 157 (4), 0–1341.
USEPA, 1989. Risk assessment guidance for superfund. In: Human Health Evaluation Manual (Part A). EPA/540/1-89/002. vol. 1. Environmental Protection Agency, Washington, DC, pp. 35–52.
Wang, S., Feng, X., Qiu, G., Fu, X., Wei, Z., 2007. Characteristics of mercury exchange flux between soil and air in the heavily air-polluted area, eastern Guizhou, China. Atmos. Environ. 41 (27), 5584–5594.
Wang, J., Feng, X., Anderson, C.W., Xing, Y., Shang, L., 2012. Remediation of mercury contaminated sites–a review. J. Hazard. Mater. 221, 1–18.
Wang, D.D., Li, W.H., Guo, H.P., et al., 2017. Analysis of mercury accumulation in different tissues of maize. J. Shanxi Agric. Sci. 45 (6), 912–917.
Yin, R.S., Feng, X.B., Shi, W.F., 2010. Application of the stable isotope system to the study of sources and fate of Hg in the environment: a review. 25 (10), 1467–1477.
Yin, R.S., Feng, X.B., Meng, B., 2013. Stable mercury isotope variation in rice plants (Oryza sativa L.) from the Wanshan mercury mining district, SW China. 47, 2238–2245.
Yin, R.S., Feng, X.B., Chen, J.B., 2014. Mercury stable isotopic compositions in coals from major coal producing fields in China and their geochemical and environmental implications. Environ. Sci. Technol. 48 (10), 5565–5574.
Zhang, Z.D., 2016. Supply and Demand of Domestic Corn Market and Prediction of Supply and Demand in the Next Five Years. Heilongjiang Grain. pp. 19–23 (in chinese).
Zhang, H., Feng, X.B., Larsscn, T., Qiu, G.L., Vogt, R.D., 2010. In inland China, rice, rather than fish, is the major pathway for methylmercury exposure. Environ. Health Perspect. 118, 1183–1188.
Zhao, L., Qiu, G., Anderson, C., Meng, B., Wang, D., Shang, L., Yan, H., Feng, X., 2016. Mercury methylation in rice paddies and its possible controlling factors in the Hg mining area, Guizhou province, Southwest China. Environ. Pollut. 1–9.
Zheng, S.A., Wu, Z., Chen, C., Liang, J., Huang, H., Zheng, X., 2018. Evaluation of leafy vegetables as bioindicators of gaseous mercury pollution in sewage-irrigated areas. Environ. Sci. Pollut. Res. 25, 413–421.
Zhu, S.l., Zhang, Z.L., Zagar, D., 2018. Mercury transport and fate models in aquatic systems: a review and synthesis. Sci. Total Environ. 639, 538–549.